International Journal of Rock Mechanics and Mining Sciences 106 (2018) 84–95

Contents lists available at ScienceDirect

International Journal of Rock Mechanics and Mining Sciences

journal homepage: www.elsevier.com/locate/ijrmms

A discontinuum modelling approach for investigation of Longwall Top Coal Caving mechanisms

Tien Dung Le[a], Joung Oh[a,*], Bruce Hebblewhite[a], Chengguo Zhang[a], Rudrajit Mitra[b]

[a] School of Mining Engineering, UNSW Sydney, NSW 2052, Australia
[b] School of Mining Engineering, University of the Witwatersrand, Johannesburg 2050, South Africa

ARTICLE INFO

Keywords:
Longwall Top Coal Caving
Discontinuum modelling
Caving mechanism
Top coal cavability

ABSTRACT

This paper presents a discontinuum modelling approach to investigate Longwall Top Coal Caving (LTCC) behaviour including stress distribution, coal and rock failures, top coal caving and roof strata rupture, and to analyse the impact of overburden movement on top coal caving. The current model ia successful in using plastic material in a discontinuum code for intact rocks. The model scale is large enough to capture the critical features of LTCC, including steady-state caving of top coal and repeatable periodic weighting of roof strata. The applicability of the numerical model was assessed by calibration with field measurements obtained from a longwall mine site. The numerical study found that the stress distribution caused by LTCC mining is in general similar to that caused by conventional longwall mining; top coal predominantly fails in shear whereas roof rock mostly fails in tension; top coal starts to cave in stress caving while main roof strata first rupture in crushing mode; and roof strata weightings periodically increase and decrease top coal cavability. The findings of this study should assist engineers in better understanding fundamental rock mechanics associated with LTCC, identifying key geotechnical parameters dominating caving behaviour, and managing top coal productivity and mine safety involved in LTCC operation.

1. Introduction

Longwall Top Coal Caving (LTCC) is considered one of the most efficient methods for mining thick coal seams.[1] The LTCC method divides a thick coal seam into two sections including lower or cutting section and upper or top coal section. The lower section is mined by the conventional longwall method while the top coal section is typically extracted by means of caving under the impact of gravity (Fig. 1).[2] Compared to other longwall methods such as Multi-Slice Longwall and High Reach Single Pass Longwall, LTCC can offer significantly reduced operational cost, high production and resource recovery rate, and improve mine safety.[3] An efficient evaluation of LTCC applicability is practically important to the coal industry. In this paper, a thick coal seam is defined as a seam having thickness in excess of 4.5 m, as based on the Australian mining practice.[1]

Successful evaluation of LTCC applicability is heavily dependent on the understanding of the important geotechnical mechanisms including stress distribution, coal and rock failures, top coal caving and roof strata movement that may result in technical risks such as face/roadway/support instability, increased surface subsidence, windblast and severe weighting events. A sufficient insight into these mechanisms is important for efficiently managing potential risks, improving mine safety and maintaining scheduled production of an LTCC operation.

LTCC-associated mechanisms have been analysed in previous studies; however, they have not been understood to a satisfactory level. In a few studies, the fundamental LTCC behaviours including stress distribution and roof strata movement were not directly investigated but were assumed to be similar to those in conventional longwall mining.[4,5] In practice, the increased mining height in LTCC may change the distribution of front abutment stress and magnitude of overburden movement from those in the conventional longwall method. In other studies, although the stress distribution and top coal failure were directly investigated, the roof strata movement and explicit top coal caving were not analysed.[6–8] In addition, the rock caving was assumed to be controlled by discontinuity failure but without intact rock failure; realistic rock caving was not sufficiently captured.[9–11]

One main reason for the limited understanding of LTCC behaviours is partly due to the difficulties in numerical modelling in past studies. Although the previous studies were useful in improving general understanding of the behaviours, they were unable to sufficiently investigate stress distribution by explicitly modelling rock caving and roof strata movement. For example, continuum modelling methods are

* Corresponding author.
E-mail address: joung.oh@unsw.edu.au (J. Oh).

https://doi.org/10.1016/j.ijrmms.2018.04.025
Received 6 October 2017; Received in revised form 9 April 2018; Accepted 10 April 2018

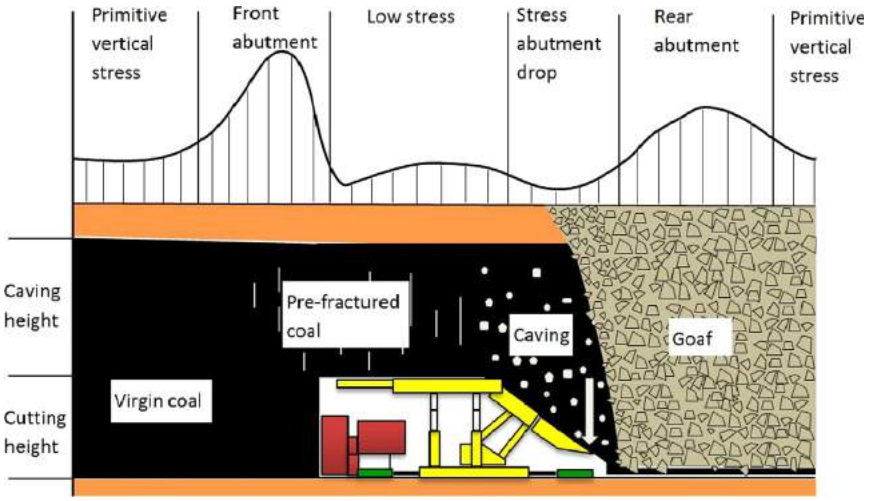

Fig. 1. Conceptual model of Longwall Top Coal Caving.[2]

capable of analysing stress distribution and rock failure; however, they require a well-developed algorithm to implicitly represent caving progress, goaf consolidation and continuous mining.[12–14] Discontinuum modelling methods with the assumption of elastic material, despite being used to explicitly model coal and rock caving, could not simulate intact rock failures in the models.[9–11] Hybrid modelling methods, meanwhile, show very limited application at present[15] mostly due to the complexity of mechanical coupling scheme between codes. For a more detailed review of the application of numerical methods in LTCC studies, readers are referred to Le et al.[3] It is noted that the advanced Extended Finite Element Method[16,17] and more recent meshless numerical methods such as Peridynamics[18–20] and General Particle Dynamics,[21–23] which are capable of realistically modelling the initiation, growth and coalesence of cracks in rock, can also be applied to investigate the LTCC-associated behaviours.

In this paper, a detailed discontinuum modelling analysis was performed by using plastic material for intact rocks in a field-scale LTCC model. The field measurements at a real LTCC face were used to calibrate and validate the proposed model. The LTCC model was then employed in detail to investigate stress distribution, coal and rock failure modes, top coal caving mechanism and roof strata rupture mode in LTCC mining. The impact of overburden movement on top coal caving was also analysed in this paper.

2. Numerical modelling approach

The Universal Distinct Element Code (UDEC)[24] which is a two-dimensional program based on Discrete Element Methods (DEM) has been used to develop a field-scale LTCC model in this paper. The discontinuum UDEC code is capable of explicitly modelling large-scale movement of roof rock strata, and complete detachment and rotation of top coal in caving. As a medium in UDEC is divided into blocks, the fracture development is closely related to the block shape and size. Accordingly, the blocks should be modelled based on field observations to overcome this limitation. The face advance along panel length has been sufficiently modelled to generate a steady-state caving of top coal under periodic weighting of roof strata, which has not been considered in most of past LTCC studies. The model has, for the first time in LTCC research, successfully used strain-softening material in discontinuum code for intact rocks. This enables all rock material failure, rock strength disintegration and rock caving to be explicitly represented in one model, which has not been possible in all previous LTCC investigations. The progressive mining, which largely contributes to successful caving of top coal, has been realistically simulated as well.

Since UDEC is a two dimensional code, the three-dimensional geometry of a geological structure cannot be represented except for special orientations. However, in longwall mining, the face advance along panel length is much greater than the face advance along panel width. Hence, a UDEC model with the plane-strain condition, which represents an LTCC face advancing along panel length and located at mid-panel width, is capable of identifying fundamental rock responses caused by LTCC. It should be mentioned that in longwall mining, groundwater may facilitate the mining-induced fracturing, opening of natural joints, bed separation and rock caving.[5] Therefore, groundwater in such discontinuities reduces the normal effective stress and in turn reduces the potential shear resistance and ultimate rock mass strength. At the mine site in this study, however, the strata in general are dry and the water has not been reported as a significant issue. The impact of groundwater on caving is thus not incorporated into the model, but recommended for separate investigations. The development of the LTCC model is described in the following sub-sections.

2.1. Geo-mining conditions at Mine A

The LTCC model is based on one LTCC face in the Bowen Basin, Queensland, Australia. Owing to confidentiality matters, the name of the mine is not disclosed and is named “Mine A” in this paper. Mine A extracts the Goonyella Middle Seam, which has a depth of 80–300 m and an average seam dip of three degrees at the site.[4,25] According to Gillam,[26] there are three stratigraphic units including coal, overbank and distributary channel units at the mine (Fig. 2). The coal unit comprises seams up to 10 m thick of banded coal with thin stone bands. The overbank unit consists of layered siltstone, shale and carbonaceous shale. The distributary channel unit comprises sandstone deposited in amalgamated distributary channels. The mechanical stratigraphy controls the occurrence, height and spacing of joints at the mine. The dominant vertical joints set strikes east-west ± 20°. The joint spacing is proportional to joint height with a spacing-to-height ratio ranging from 0.7 to 1. Joints are most dense in coal seams and least dense in amalgamated channel units. At the Bowen Basin, the predominant orientation of the maximum horizontal stress is north-northeast.[27] At the study site, the maximum horizontal stress is 1.4–2.4 times the vertical stress.[4,26]

The field measurements at Mine A refer to the coal seam recovery rate, top coal caving distance, immediate roof caving distance and load on face support. The LTCC operation was considered successful with a seam thickness recovery rate of up to 85%.[28] According to Mine A engineers (Coutts B and Payne D, personal communications), the top coal started to cave at 8–10 m of face advance out of installation room. By 20 m of face advance, the goaf formed full width of the face

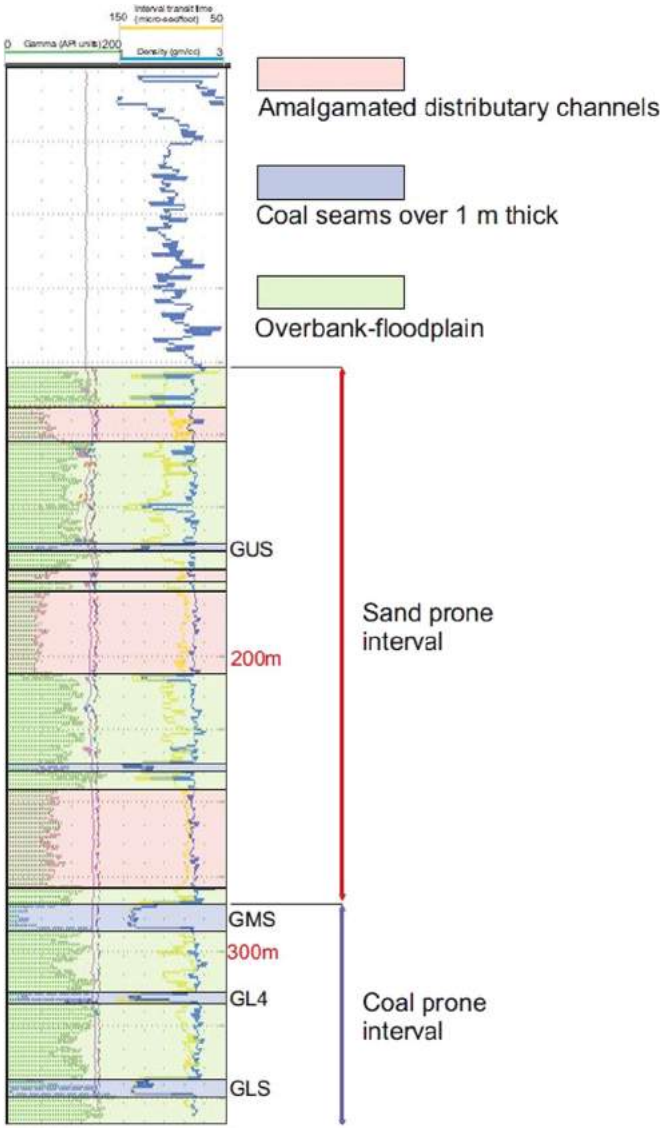

Fig. 2. Stratigraphic sequence at Mine A.[26]

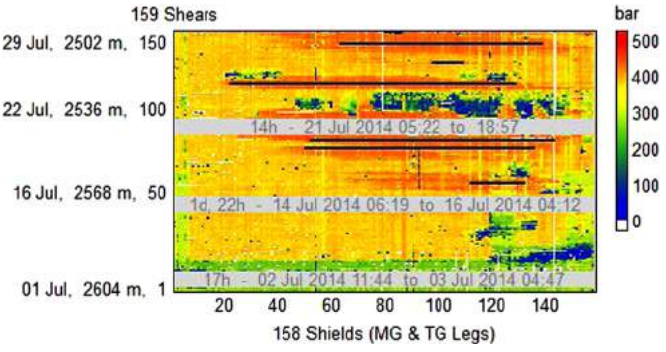

Fig. 3. Time-Weighted Average Pressure map in the first 100 m of extraction at Mine A.

including stones from immediate roof. The load on face support was monitored using Longwall Visual Analysis (LVA).[29] From the LVA data, the weightings and cavity risks within the first 100 m of extraction were extracted and are displayed through the Time-Weighted Average Pressure (TWAP) map in Fig. 3. As can be seen from the figure, the first weighting (black line) and the major cavity risk (blue area) along the panel length and at the mid-panel width occurred at approximately 60 m and 70–75 m of face advance, respectively. It is important to know that in October 2015, a severe weighting occurred and took the face several weeks to restart production.[30] The impact of roof weighting on LTCC performance is thus important and needs to be investigated.

2.2. Model configuration

The model has a total height of 250 m representing the entire overburden strata and floor strata at Mine A. The total length of model is 1200 m, which is five times the length of mining area (Fig. 4). This 240 m length of mining area was aimed to achieve the periodic weighting of roof strata. The side boundaries were fixed in X direction while the bottom boundary was fixed in Y direction, representing the roller boundary condition.[24] The model has six major strata including floor, coal seam, immediate roof, Main Roof 1, Main Roof 2 and upper strata. Note that Main Roof 1 is representative of the thickest sandstone strata at the site. The areas of interest including coal seam, immediate roof, Main Roof 1 and Main Roof 2 were modelled with sufficient detail of geological structures. The bedding spacing and vertical joint spacing in top coal are equal to 0.5 m, based on the size of caved materials at the mine. Meanwhile, those spacings in Main Roof 1 are equal to 3 m, representing moderately bedded sandstone. The vertical stress is at a rate of 2.5 MPa per 100 m cover depth while the horizontal stress was assumed to be two times the vertical stress. The LTCC model consists of 9258 blocks and 93,072 diagonally opposed triangular elements. The diagonally opposed triangles improve the accuracy of calculation for the failure and collapse of intact materials. A greater number of elements improve plastic collapse calculation while simultaneously decrease calculation speed.[24] Thus, to obtain an accurate simulation of rock failure and caving within realistic time constraints, each block in the areas of interest was discretised into more elements compared to that in other areas. The model takes approximately four months to complete the extraction.

2.3. Material constitutive model

All coal and rocks in the LTCC model were simulated using UDEC plastic materials. The areas of interest consist of strain-softening materials to capture the rock strength disintegration. The strain-softening material model is based on the Mohr-Coulomb model with non-associated shear and associated tensile flow rules.[24] After the onset of plastic yield, the strain-softening model assigns softening/hardening behaviours to materials through prescribed variations of the Mohr-Coulomb model properties. The cohesion, friction, dilation and tensile strength may soften/harden as functions of softening/hardening parameters measuring the plastic strain. The shear softening/hardening parameter (e^{ps}) has an incremental form defined in Eq. (1). The tensile softening/hardening parameter (e^{pt}) measures the accumulated tensile plastic strain with its increment defined in Eq. (2).

$$\Delta e^{ps} = \left\{\frac{1}{2}(\Delta e_1^{ps} - \Delta e_m^{ps})^2 + \frac{1}{2}(\Delta e_m^{ps})^2 + \frac{1}{2}(\Delta e_3^{ps} - \Delta e_m^{ps})^2\right\}^{\frac{1}{2}} \quad (1)$$

$$\Delta e^{pt} = \Delta e_3^{pt} \quad (2)$$

where $\Delta e_m^{ps} = \frac{1}{3}(\Delta e_1^{ps} + \Delta e_3^{ps})$; $\Delta e_j^{ps}, j = 1, 3$ are the principal plastic shear strain increments; and Δe_3^{pt} is the increment of tensile plastic strain in the direction of the major principal stress.

All discontinuities including vertical joints and bedding planes in the LTCC model were modelled using the UDEC Coulomb slip model. This basic joint material model is the generalisation of the Coulomb friction law.[24] The discontinuities are allowed to fail in shear and tension. In the elastic range, the discontinuity behaviour is controlled by its normal and shear stiffness.

It is noted that in past LTCC studies, the UDEC models have been

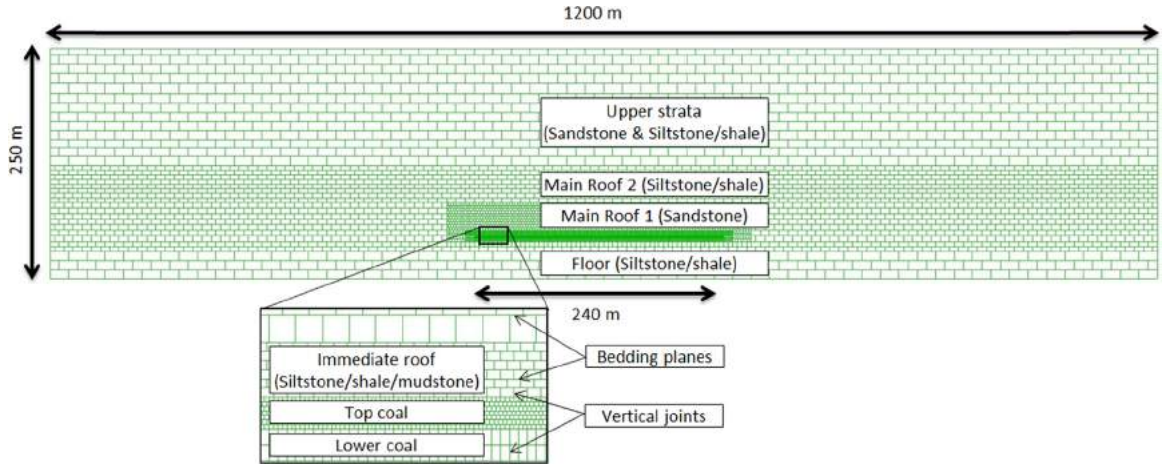

Fig. 4. Configuration of UDEC LTCC model.

limited in modelling coal and rock blocks as elastic materials. Poulsen[9] believed that the interaction between intact block failure and joint failure could result in extremely complex material response. A similar problem was identified during the development of the current model and was addressed in the next section.

2.4. Material properties

No rock sample from Mine A was collected and tested in this study due to limited access. The intact Uniaxial Compressive Strength (UCS) values of typical rocks at the mine and at its neighbouring mines are available in several studies.[4,31–34] For example, coal UCS, immediate rock UCS and sandstone UCS range from 8.7 to 12.26 MPa, 10–30 MPa and 15–50 MPa, respectively. The properties of geological structures at Mine A are found in a few studies.[35,36] A series of field investigations at the neighbouring mines found that the bedding planes have a friction angle ranging from 12 to 30 degrees.[37]

The properties of coal and rocks for the modelling are shown in Table 1. The intact UCS value of materials was scaled to field value (UCS^*) using a reduction factor of 0.58. This factor was commonly applied for the Bowen Basin rocks.[37,38] The elastic modulus (E^*) in GPa was 0.31 times the UCS^* value in MPa, as suggested by Wilson.[39] The Poisson's ratio (ν) was assumed to be 0.25, which was suggested for most coal measure lithologies.[39,40] The cohesion value (C) was derived from the UCS^* value and the friction angle (ϕ), using the Mohr-Coulomb failure criterion.[24] The tensile strength (σ^t) was assumed to be one tenth of the UCS^* value.[40] The critical shear strain of coal, which is required for reduction of shear strength from peak to residual value, was adapted from past numerical models of coal measure rocks.[14,41] The critical shear strain of rock is commonly smaller than that of coal due to the more brittle behaviour in hard rock. The critical tensile strain was assumed to be equal to the critical shear strain (ε^p) in each rock type due to limited guideline.[42]

There are a few guidelines for the determination of post-peak strength properties.[43–45] In the current study, the residual cohesion strength (C_r) was assumed to be 20% of its peak strength. The friction angle was kept unchanged through failure of material, which was also assumed in several studies.[46–48] The post-peak tensile strength has been widely assumed to be zero in numerical models. In UDEC, however, this assumption can lead to model instability due to the large tensile strain of intact blocks after failure. The problem becomes more serious when complete detachments of blocks are possible. Such a model problem was identified through preliminary modelling tests and discussions with UDEC developers (Wines D, personal communication). On the other hand, it is possible to assume that during the caving in a UDEC model, the failed rock mass can maintain a small residual tensile strength (Wines D, personal communication). Therefore, the residual tensile strength (σ_r^t) was assigned to 10% of its peak strength in the current model, based on the similar assumption in a past study.[49]

The properties of discontinuities for the modelling are shown in Table 2. In UDEC simulation of rock caving, a high discontinuity stiffness results in less caving whereas a low discontinuity stiffness results in greater caving.[4] For the current model, the possible values of stiffness were first estimated using Eqs. (3) and (4), as suggested by Itasca.[24] A series of models were then run to refine the discontinuity stiffness in coal seam in conjunction with caving behaviour and solution time. For simplicity of modelling, the discontinuity stiffness in other strata was assumed to be equal to that in the seam. A ratio of normal to shear stiffness of 10 was used.[50,51] The tensile strength and cohesion of discontinuities were assumed to be zero. The friction angle of discontinuities in coal seam was less than that in rock strata in the model.

$$k_n \text{ and } k_s \leq 10\left[max\left[\frac{K+\frac{4}{3}G}{z}\right]\right] \tag{3}$$

$$\frac{\sigma}{k_n} \leq 0.1z \tag{4}$$

where k_n and k_s are the normal and shear stiffness of discontinuities; K and G are the bulk and shear moduli of block material; z is the width of the zone adjoining the discontinuity; and σ is the typical stress in the system.

Table 1
Coal and rock properties in UDEC LTCC model.

Rock units	UCS*(MPa)	E*(GPa)	ϕ (^{0})	C (MPa)	σ^t (MPa)	C_r (MPa)	σ_r^t (MPa)	ε^p (%)
Sandstone	26.62	8.25	42	5.92	2.66	1.18	0.26	0.1
Siltstone/shale	17.40	5.39	34	4.62	1.74	0.92	0.17	0.1
Siltstone/shale/mudstone	11.60	3.59	34	3.08	1.16	0.61	0.11	0.1
Coal	6.64	2.05	30	1.91	0.66	0.38	0.06	0.5

Table 2
Discontinuity properties in UDEC LTCC model.

Rock strata	Normal stiffness (GPa/m)	Shear stiffness (GPa/m)	Cohesion (MPa)	Friction (degree)	Tensile strength (MPa)
Roof and floor	100	10	0	25	0
Immediate roof	100	10	0	20	0
Coal seam	100	10	0	15	0

2.5. Progressive mining

The progressive mining in the LTCC model was simulated in a way that is similar to the mining progress in reality. The first step is to extract the seam by cutting one metre in the lower coal section. This small interval in extraction also minimises the transient effect of inertial reaction caused by the sudden cutting/deletion in the model response. The second step is to advance the face support by one metre by deleting the support at the old position and setting it again at the new face position. The third step is to run the model to reach equilibrium state. The last step is to recover the top coal by deleting the caved blocks located within the recovery area. After the mining cycle is complete, the next cycle will repeat the steps. All the mining tasks were implemented in the UDEC model using a built-in programming language (FISH).

The interaction between face support, top coal and surrounding rocks contributes to the roof rocks' behaviour. Hence, a realistic simulation of face support is required. In the current model, a set of support members available in UDEC was used to cover a space of 4.5 m, representing a practical length of roof canopy.[52] The spacing between two adjacent members is sufficiently small to avoid any blocks caving inside. The tip-to-face distance was assumed to be 0.4 m. The recovery area is located within 2.5 m behind the face support, simulating a real window in rear canopy. The support members were assigned with realistic values of setting pressure, yield pressure and stiffness (Table 3). It is noted that these values were scaled down as the default support width in the out-of-plane direction in UDEC is 1 m. Furthermore, a very high force of the support members can be activated to avoid any excessive support instability.

2.6. Model indicators

Five indicators were developed and monitored during the progressive mining in the LTCC model. The indicators are "Load on face support", "Front abutment stress", "Mode of failure", "Maximum subsidence" and "Top coal recovery rate". The load on face support was measured through the total force exerted by the support members. The value of the force was obtained using a UDEC command. The force was recorded in every face advance when the model was in equilibrium. The front abutment stress was monitored in both lower coal and top coal sections. There are two ways of monitoring the stress. Firstly, the vertical stress was plotted along two horizontal lines located in the middle of the lower coal (line A) and in the middle of the top coal (line B). Secondly, the magnitudes of vertical stress at locations 10 and 15 m ahead of the face line and in the middle of lower coal and top coal thicknesses were monitored using a FISH function. These lines and locations (black dots) are illustrated in Fig. 5. The mode of intact block failure was monitored through the numbers of zones that failed in tension and in shear, using another FISH function. The ratio of the number of zones failed in tension to the number of zones failed in shear was calculated using Eq. (5). The maximum subsidence of the model

Table 3
Force-displacement relationship of support members in LTCC model.

Force (MN)	0	5.16	6.45	6.45	100
Displacement (m)	0	1e−4	0.01	0.2	≥ 0.3

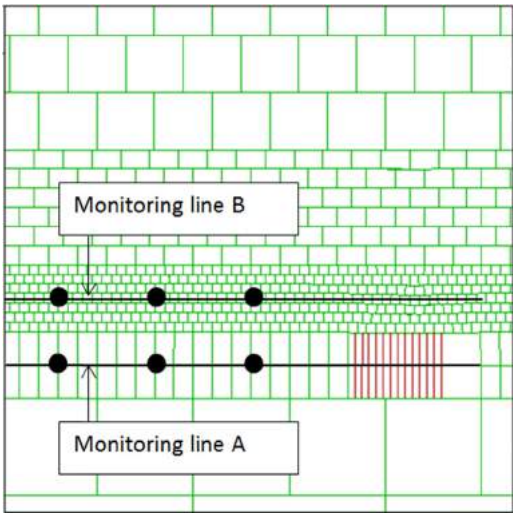

Fig. 5. Monitoring of front abutment stress.

surface was recorded after every 10 m of face advance using a UDEC command. The top coal recovery rate was measured in every 10 m of face advance and not incrementally (TCR_{10}), as described in Eq. (6).

$$Tension - to - shear\ ratio = \frac{Number\ of\ zones\ failed\ in\ tension}{Number\ of\ zones\ failed\ in\ shear} \quad (5)$$

$$TCR_{10} = \frac{The\ number\ of\ top coal\ blocks\ recovered\ in\ every\ 10\ m\ of\ face\ advance}{The\ number\ of\ pre - mining\ top\ coal\ blocks\ in\ every\ 10\ m} \quad (6)$$

2.7. Model validation

The LTCC model was calibrated against the first caving distance of top coal (the interval from the face entry to a face line where top coal starts to cave) observed at Mine A. The model was further validated by comparing the movement of roof strata and the load on face support to those measured in the field. The immediate roof started to cave at 23 m while the first rupture (or first weighting event as discussed in the next paragraph) of main roof occurred at 73 m of face advance. These distances were within 82% of the field measurements, indicating a good agreement.

The computed load and field load on face support in the first 120 m of extraction are shown in Fig. 6. The field load was derived from the average leg pressure of a support located in the middle of panel width.

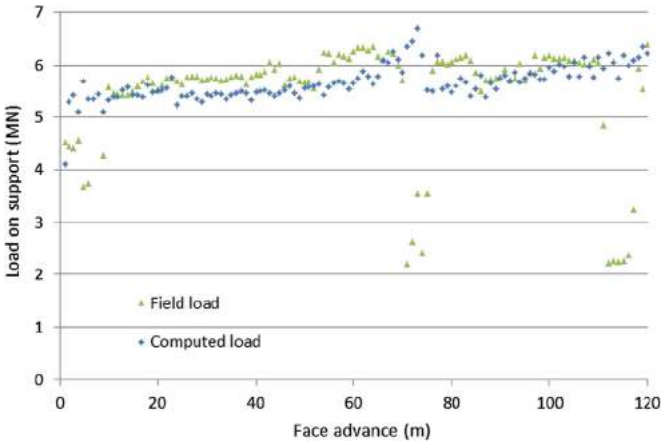

Fig. 6. Computed load and field load on face support.

The field load was also scaled down to correspond to 1 m width of the UDEC support in the out-of-plane direction. As can be seen from Fig. 6, the variation of the computed load followed a similar trend to that of the field load. In the initial face advances, the calculated load showed an increasing trend. However, this load decreased in the next few cuts when the top coal started to cave. The calculated load also increased before the first caving of immediate roof and then quickly decreased after this caving. During the periodic caving of top coal and immediate roof, the load followed slight fluctuations. When the face advanced about 60 m, the calculated load increased markedly. This is due to the increasingly downward sagging of main roof strata. The rocks in main roof strata started to fail at 67 m of face advance and this increased the support load significantly. After the first rupture of main roof strata, which was at 73 m of face advance, the load dropped rapidly. The significant increase and rapid drop in the computed load also indicates that the first weighting of main roof strata is formed and related to their first rupture. In the subsequent face cuts, the load followed another increasing trend, denoting the next sagging of overlying strata.

3. Model results and discussion

3.1. Stress distribution

The distributions of principal stresses at different stages of mining in the LTCC model are shown in Fig. 7. Note that before the model extraction, the vertical and horizontal stresses denoted the minor and major principal stresses, respectively. Due to the extraction, the vertical stress was relieved above and below the mined-out area whereas it concentrated in the unmined coal (abutment stress). With the face advancing, the area of vertical stress relief and the abutment stress also increased. The horizontal stress, from the start of the extraction, continued to concentrate in the immediate roof and main roof. When the strata failed, the horizontal stress was significantly released; however, it could still be transmitted in the broken but un-caved strata. The model results indicate that the stress distribution caused by LTCC mining is in general similar to that caused by conventional longwall mining.[53] The similarity is due to the fact that LTCC uses the conventional longwall method for extracting the lower coal section.

It is also observed from these figures that in the unmined coal seam ahead of the face line, the direction of minor principal stresses changed from vertical to horizontal or nearly horizontal. Meanwhile, the direction of major principal stresses changed from horizontal to vertical or inclined. The changes are due to the concentration of vertical stress combined with the relief of horizontal stress in this area. Further into the unmined seam, the directions of principal stresses gradually returned to their pre-mining state. In cases where the pre-mining major principal stress is vertical, the change in direction may occur above and below the mined-out area.[41]

The vertical stress was plotted along the monitoring lines in Fig. 7 as well. The horizontal blue line A and the horizontal red line B were 1.75 and 5.25 m above the seam floor, respectively. The magnitude and location of peak abutment stress are displayed at every 20 m of face advance in Fig. 8. The model results suggest that as the LTCC face advances, the peak abutment stress increases in magnitude while its location moves far away from the face line. After 220 m of extraction, the peak abutment stress in the lower coal and top coal sections corresponded to 2.67 and 2.94 times the pre-mining stress. Simultaneously, the peak abutment stress reached 12–13 m ahead of the face line.

The computed abutment stress is compared to that in similar numerical analyses of an Australian conventional longwall[54–56] and a Turkish LTCC face.[7] It was found in the Australian face that the maximum abutment stress was twice the overburden stress and occurred about 10 m ahead of the face. These model results were likely obtained at 120 m of face advance. In the current model and at the same face advance, the peak abutment stress in the top coal was 1.94 times the pre-mining stress and occurred 8 m ahead of the face. This agreement is because the major principal stress was horizontal and at least two times greater than the vertical stress in both studies. Alternatively, it was found in the Turkish face that at 150 m of face advance, the peak abutment stress was 2.5 times the initial field stress and occurred 7 m away from the face. In the current model, the corresponding values were 2.16 times and 8 m, respectively. The ratio of peak abutment stress to pre-mining stress is 13.6% lower than that from the Turkish face. The main reason is that in the Turkish face, the major principal stress was vertical rather than horizontal. Note that the relief of a high horizontal principal stress into the mined-out area is quite significant and has a decreasing influence on the vertical stress.[56] The decrease impact of the horizontal stress on the peak abutment stress was therefore less significant in the Turkish face.

The changes in vertical stress at the monitoring locations are shown in Fig. 9. In the first half of the model extraction, the vertical stress measured at all locations followed an increasing trend. This means that the peak abutment stress was located within 10 m ahead of the face line. However, in the second half, the vertical stress at locations 10 m ahead of the face displayed significant fluctuations while the stress at locations 15 m showed an increasing trend. This indicates that the peak abutment stress moved beyond 10 m but still within 15 m ahead of the face. For all locations and at a face advance of 70–75 m, there was a marked drop in vertical stress. This drop confirms that the first weighing was formed and accompanied by the first rupture of main roof strata.

3.2. Material failure

The failure state of discontinuities at the end of the extraction in the LTCC model is displayed in Fig. 10. The discontinuities that have opened (tensile failure) are in red colour and those that have slipped (shear failure) are in blue colour. As can be seen from the figure, the failure of discontinuities developed upward to the model surface, downward into the model floor and to a certain distance ahead of the face line. The discontinuities failed in both tension and shear. In the top coal, shear failure mainly developed along the bedding planes while tensile failure largely occurred along the vertical joints. In the main roof strata, shear failure happened in the area above the support while tensile failure occurred along bed separations above the goaf area. In the upper strata, both slip and separation of beddings were observed. It is noted that the assumption of discontinuities with zero tensile strength and zero cohesion may facilitate the development of the failure in the model.

The failure state of intact rocks at the end of the extraction is displayed in Fig. 11. The blocks that fail in current shear, past shear and tension are illustrated by red star *, green X and purple o, respectively. As can be seen from the figure, the roof rocks failed up to 160 m above the seam floor. The micro-seismic measurement at Gordonstone Mine (now Kestrel) in the Bowen Basin indicated that rock fracture occurred up to 100 m above the coal seam.[55] This result was likely obtained within 120 m of face advance at this mine. In the current model and at the same face advance, the roof rocks failed up to 83 m above the seam floor. It is noted that the depth of cover at Gordonstone Mine is similar to that at Mine A. The model result therefore agrees with the field measurement. On the other hand, the tension-to-shear ratio was recorded at every 5 m of face advance and for the top coal and Main Roof 1. It was found that shear failure was the predominant mode in the top coal. In contrast, tensile failure was the controlling mode in the main roof strata. The failure mode in top coal is in accordance with that analysed by Yasitli and Unver.[7]

The failure modes of discontinuities and intact blocks can be explained by the interaction of material strength with stress distribution. In a normal mining cycle and in the top coal immediately above the support, the horizontal stress is considerably released. Meanwhile, the vertical stress still acts owing to the weight of overlying strata and the

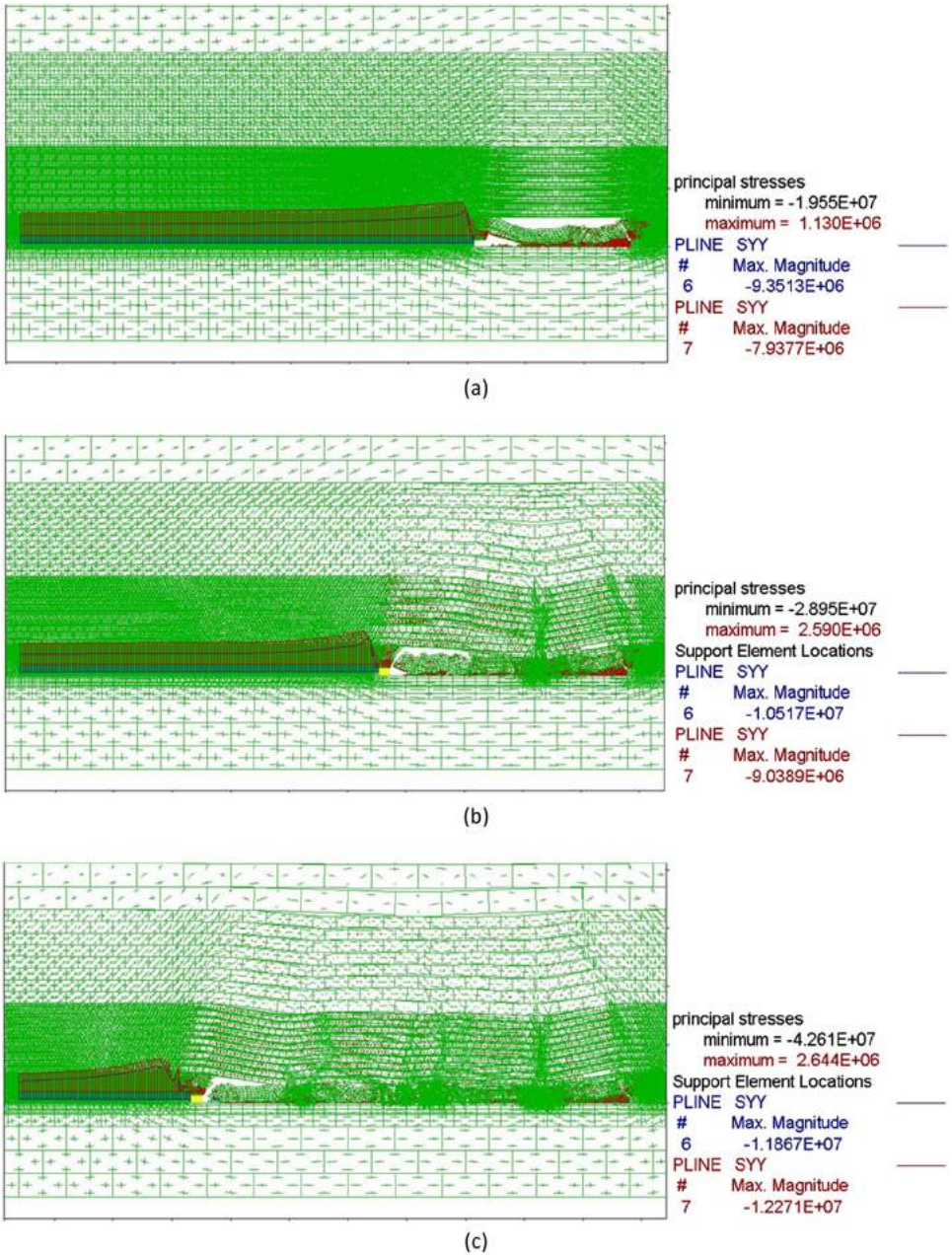

Fig. 7. Principal and abutment stresses at different stages of mining. (a) 60 m, (b) 100 m and (c) 180 m.

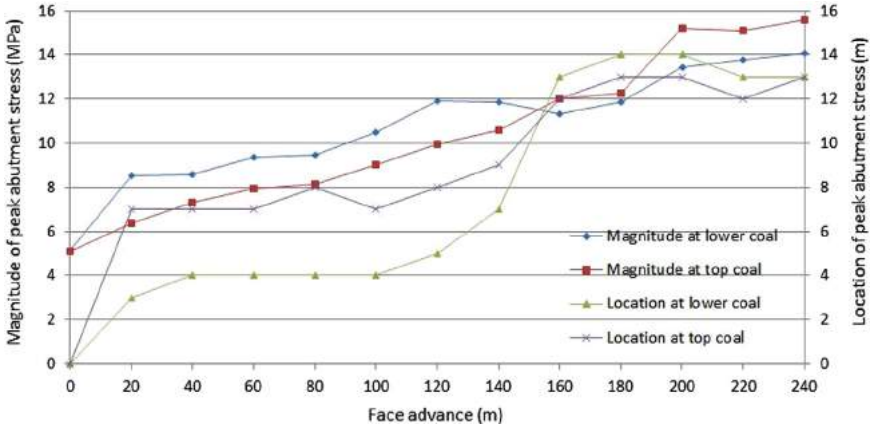

Fig. 8. Changes in peak abutment stress at every 20 m of face advance.

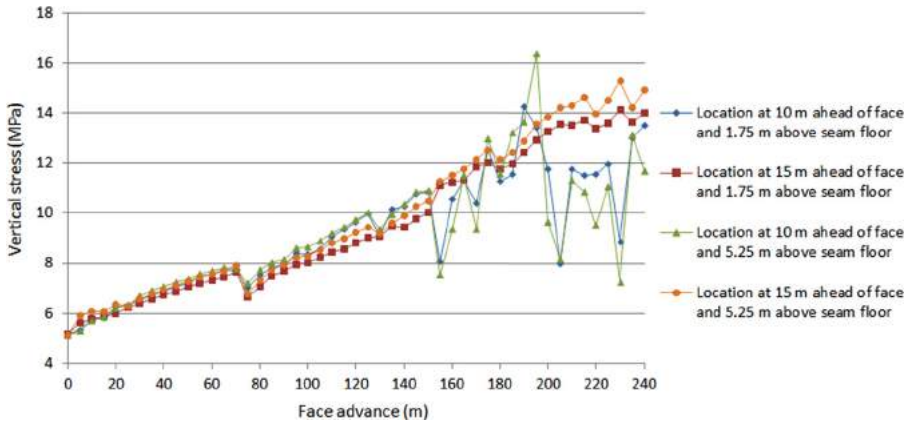

Fig. 9. Changes in vertical stress at monitoring locations.

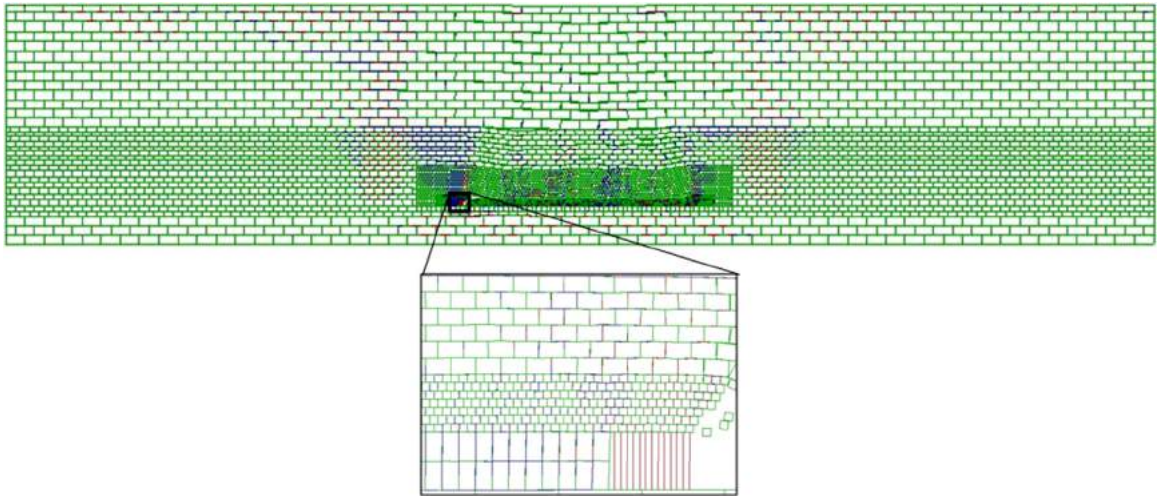

Fig. 10. Failure of discontinuities at 240 m of face advance (tensile and shear failures are in red and blue, respectively). (For interpretation of the references to color in this figure legend, the reader is referred to the web version of this article.)

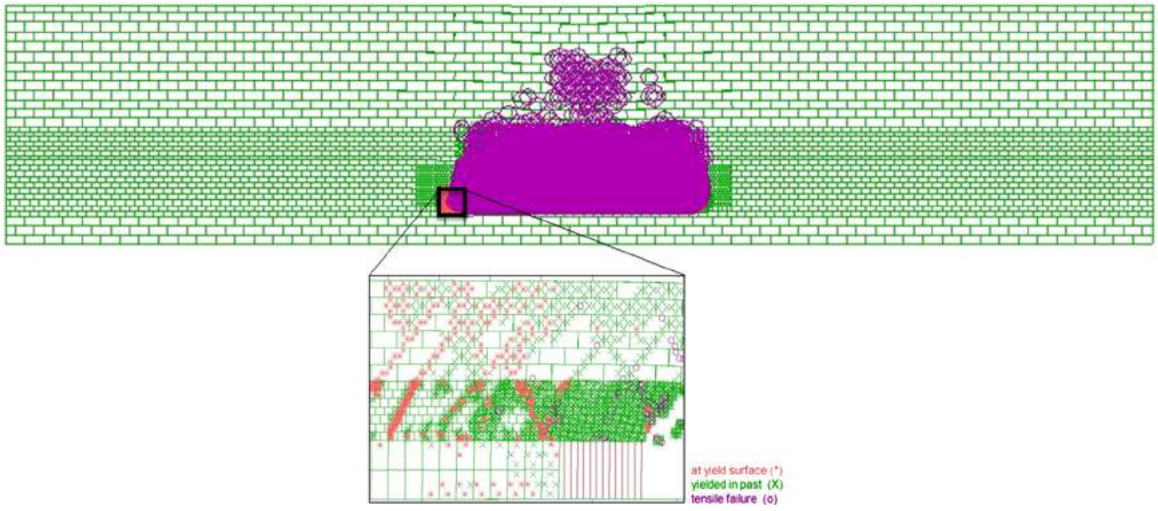

Fig. 11. Failure of intact rocks at 240 m of face advance. (For interpretation of the references to color in this figure, the reader is referred to the web version of this article.)

force from the support. This area is considered in low confining stress. In this condition, coal mass can fail in tension along the vertical joints (Fig. 10). At the same time, the minor principal stress, which is horizontal or nearly horizontal, becomes tensile. If this induced-tensile stress exceeds the tensile strength of intact coal, coal blocks will fail in tension. Further into the unmined seam, the confining stress becomes greater and that causes intact blocks and discontinuities to predominantly fail in shear. In the main roof strata and immediately before the first rupture, some zones in roof rocks failed in tension in the middle and at both ends of the bridging strata (Fig. 12(a)). In the middle of the

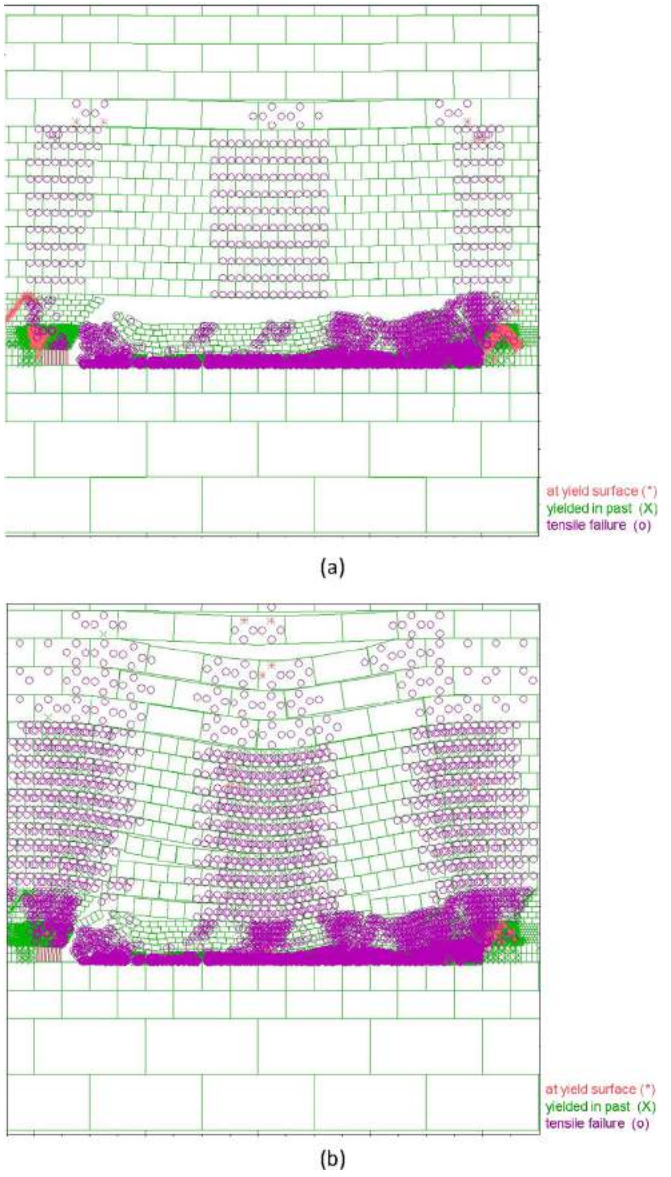

Fig. 12. Rock blocks failure. (a) Immediately before and (b) after the first rupture of strata.

strata, the relief of vertical stress and the concentration of high horizontal stress can induce the minor principal stress to be tensile. When this tensile stress exceeds the tensile strength of rock, tensile failure

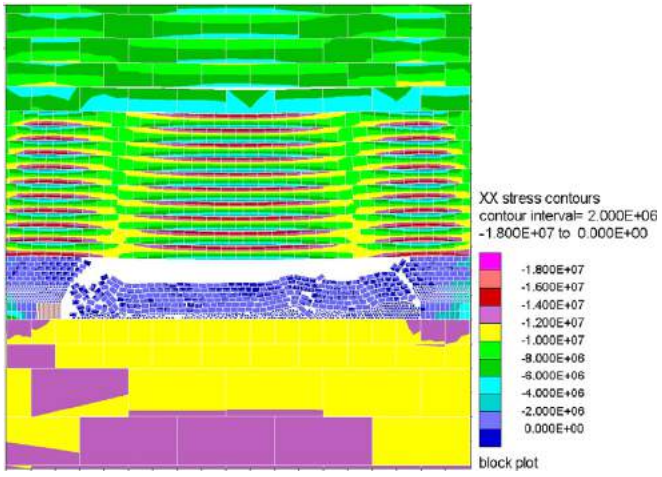

Fig. 14. Distribution of horizontal stress immediately before the first rupture of strata.

occurs in this area. The tensile failure at the two ends, however, is due to the concentration of nearly vertical stress while the horizontal stress is relieved because of the strata sagging. After the first rupture, the roof strata above the support can continue to predominantly fail in tension (Fig. 12(b)).

3.3. Top coal caving and strata rupture

From the LTCC model, a state of failure in the top coal before its first caving is shown in Fig. 13. Because an amount of horizontal stress could still be transmitted through this section, the top coal remained stable in the current cut and then caved at 8 m of face advance under the impact of gravity. As can be seen, the top coal failed in both intact blocks and discontinuities. The mechanism of the first caving of top coal in this case can be attributed to stress caving.[47]

The progressive movement of overburden strata showed that the main roof bridged over a long distance of face advance and then ruptured at a face advance of 73 m. This stability can be explained by the formation and failure of voussoir beams in the strata. The voussoir beam theory has been applied to explain the stability of horizontally laminated and vertically jointed rocks above an underground excavation.[57] The theory suggests that in the upper portion of a beam, the beam deflection will result in compressive stress. Meanwhile, in the lower portion, the deflection may result in compressive or tensile stress depending on the magnitude of the in-situ stress.[58] For the current LTCC model, as the mining started and progressed, the strong rocks in main roof strata could remain intact. The roof strata started to separate along the bedding planes while the blocks rotated and interlocked each

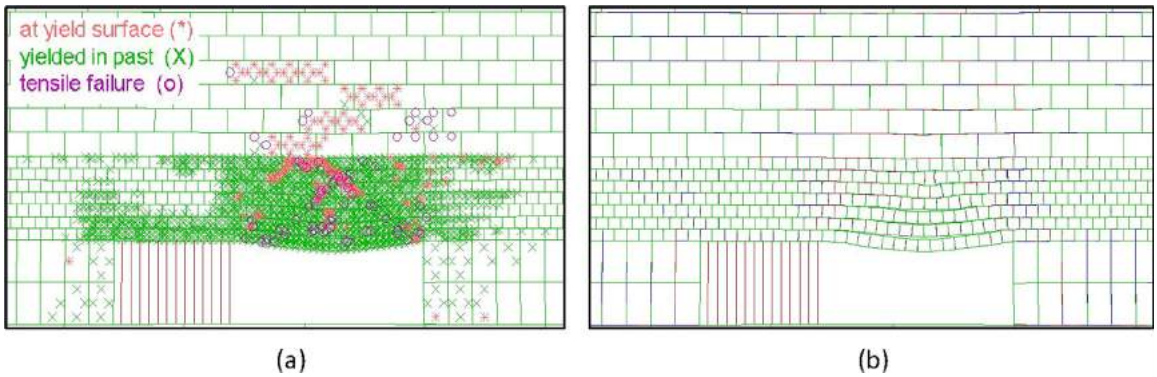

Fig. 13. Failure in top coal before the first caving. (a) Block failure and (b) discontinuity failure (tensile and shear failures are in red and blue, respectively). (For interpretation of the references to color in this figure legend, the reader is referred to the web version of this article.)

Table 4
Maximum subsidence after every 20 m of face advance.

Face advance (m)	20	40	60	80	100	120	140	160	180	200	220	240
Subsidence (m)	0.00	0.01	0.03	0.03	0.06	0.12	0.17	0.30	0.54	0.86	1.37	1.81

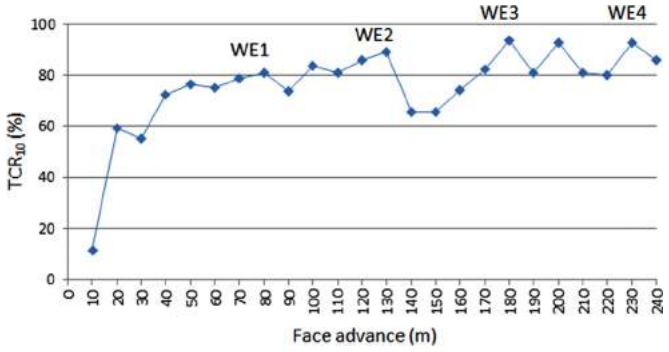

Fig. 15. Top coal recovery rate in every 10 m of face advance.

other. This resulted in the concentration of horizontal stress in the roof strata. As can be seen in Fig. 14, the high horizontal stress concentrated in the upper portion of rock stratum (one beam). In some zones in the lower portion, tensile failure occurred as discussed in Section 3.2. The voussoir beams were formed in the strata. The load from upper strata and the dead weight of beams were transferred to the abutments. The main roof strata therefore remained stable for a large face advance. The bridging strata failed when their deflection reached a limitation. According to Diederichs and Kaiser,[57] the primary failure modes of a voussoir beam are buckling (snap-through), crushing (compressive failure at the mid-span and abutments), abutment slip and diagonal fracturing. In the case of longwall mining where the ratio of mined-out span length to stratum thickness is greater than 10, a voussoir beam can fail in buckling or crushing mode. The crushing mode was observed in the LTCC model (Fig. 12(b)).

After the first rupture, Main Roof 1 and Main Roof 2 continued to bridge and rupture periodically at 128, 179 and 233 m of face advance. Simultaneously, the upper strata continued to displace downwards increasingly. The first weighting event (WE1) of main roof strata was found to be related to the first rupture, as discussed in Sections 2.7 and 3.1. Similarly, the next three weighting events (WE2, WE3 and WE4) were also found to be formed along with the periodic rupture of the main roof strata (Fig. 9).

3.4. Impact of strata movement on top coal caving

The impact of roof strata movement on top coal caving is analysed through the maximum subsidence and top coal recovery rate in the LTCC model. Steady, repeatable and realistic values of surface subsidence as the face advances denote a steady-state movement of the roof strata while the top coal recovery rate represents the cavability of top coal in every 10 m of face advance. The maximum value of surface subsidence after every 20 m of face advance is displayed in Table 4. In general, the maximum subsidence showed an increasing trend as the face advanced. The increasing trend indicates that the overburden strata did not reach their maximum possible movement. If the face progressed further, the overlying strata would continue to move downwards with greater surface subsidence magnitude. The main cause that inhibits the surface subsidence reaching its maximum possible value is the ratio of the extraction length to the cover depth. According to an empirical prediction based on the Australian geology,[59] the ratio at approximately 1.1 explains why the maximum subsidence followed an increasing trend in the current model. It is suggested that to achieve a maximum vertical movement of overburden strata along the panel length, any future UDEC model should take into account the relationship between cover depth, extraction length, strata characteristics and computing time.

The top coal recovery rate in every 10 m of face advance is shown in Fig. 15. From the face entry to a face advance of 70 m, the recovery rate followed a significantly increasing trend. This trend is associated with the progressive caving of top coal and immediate roof, and with the increasing sagging of the bridging roof strata. Along with the formation of the first weighting, the high roof pressure at the face facilitated the failure and caving of top coal. This explains the increase in the TCR_{10} value of up to 80 m. In the next face advance of 80–90 m, the first weighting was completed. The roof pressure dropped considerably; and consequently, the TCR_{10} value also decreased in this interval. In other words, the first weighting of overlying strata has an impact on top coal cavability. The next weightings were found to periodically increase and decrease the cavability as well. Note that at the face advance of 190–200 m, the TCR_{10} value reached a high rate without any noticeable movements in the overlying strata. This anomaly indicates that top coal cavability can be significantly impacted but is not limited to roof weighting events.

The analyses of roof strata movement and associated top coal caving suggest that a steady-state caving of top coal can be achieved once periodic weighting of important main roof strata occurs. It can be seen from Table 4 and Fig. 15 that while the upper strata continued to move downwards, the maximum TCR_{10} values were similar at approximately 93% throughout the extraction. This observation indicates that for LTCC operation, the upper strata may displace and add surcharge loads on the below strata; however, their effect on top coal cavability is less significant than the effect from the important main roof strata. It is noted that depending on roof strata characteristics and its influence on main roof behaviour, the important strata can be one or several main roofs immediately above a coal seam.

4. Summary and conclusions

This paper presents a detailed discontinuum modelling analysis using a field-scale LTCC model. The current modelling, for the first time regarding LTCC problems, successfully uses the strain-softening material in UDEC for intact rocks. The simulation explicitly represents the top coal caving and adequately captures both failure and strength disintegration of rocks involved in LTCC operation. The model scale and progressive mining simulations sufficiently induce the steady-state caving of top coal under the repeatable periodic weighting of main roof strata. The developed model, while satisfactorily simulating a large-scale strata movement, inevitably requires more computation time. With a reasonable scale of geometry, the model can be efficiently used for the cavability assessment of LTCC for a new mine site. The accuracy and reliability of the model results could be ensured through the proper determination of input rock properties and the calibration and validation of the LTCC model against field measurements.

The better understanding of the LTCC behaviours and of the impact of overburden movement on top coal caving has been considerably improved through investigations of the field-scale model's simulations. The study confirms that the stress distribution in LTCC mining is similar to that in conventional longwall mining. A high horizontal principal stress is found to reduce the magnitude of peak abutment stress and to change the direction of principal stresses ahead of the coal face. A detailed analysis of material failure provides further evidence to demonstrate that top coal predominantly fails in shear. The weighting events of roof strata are found to be related to the strata ruptures, which is consistent with past empirical studies.[60] The current study finds that

top coal starts to cave in stress caving and that changes of top coal cavability are consistent with periodical roof weightings. Additionally, the analysis suggests that a steady-state top coal caving with maximum TCR values is achieved in an LTCC mining once its periodic weighting of main roof strata occurs. The findings of this study therefore assists engineers in better understanding fundamental rock mechanics, identifying key geotechnical parameters and rock instability risks, and managing top coal productivity and mine safety involved in LTCC operation.

Acknowledgements

The Vietnam Ministry of Education and Training (MOET) and UNSW Sydney are thanked for supporting this work. Adjunct Professor Dan Payne and Mr. Bob Coutts are gratefully acknowledged for their permission of using field measurements.

Conflicts of interest

None.

References

1. Hebblewhite B, Simonis A, Cai Y. *Technology and Feasibility of Potential Underground Thick Seam Mining Methods. ACARP Project C8009*. Brisbane, Australia: UNSW Mining Research Centre; 2002.
2. Xu B. *Application of the Longwall Top Coal Caving System in Australian Thick Seam Coal Mines. Master Thesis.* Sydney: The University of New South Wales; 2004.
3. Le TD, Mitra R, Oh J, Hebblewhite B. A review of cavability evaluation in longwall top coal caving. *Int J Min Sci Technol.* 2017;27(6):907–915.
4. Vakili A. *Cavability Assessment in Longwall Top Coal Caving Technology. Ph.D Thesis.* Sydney: The University of New South Wales; 2009.
5. Galvin JM. *Ground Engineering - Principles and Practices for Underground Coal Mining.* Cham: Springer International Publishing; 2016.
6. Xie H, Chen Z, Wang J. Three-dimensional numerical analysis of deformation and failure during top coal caving. *Int J Rock Mech Min Sci.* 1999;36(5):651–658.
7. Yasitli NE, Unver B. 3D numerical modeling of longwall mining with top-coal caving. *Int J Rock Mech Min Sci.* 2005;42(2):219–235.
8. Xie GX, Chang JC, Yang K. Investigations into stress shell characteristics of surrounding rock in fully mechanized top-coal caving face. *Int J Rock Mech Min Sci.* 2009;46(1):172–181.
9. Poulsen BA. *Evaluation of Software Code UDEC for Modelling Top Coal Caving in an Australian Environment. Report 1115F.* Brisbane, Australia: CSIRO Exploration and Mining; 2003.
10. Vakili A, Hebblewhite BK. A new cavability assessment criterion for Longwall Top Coal Caving. *Int J Rock Mech Min Sci.* 2010;47(8):1317–1329.
11. Dao HQ. *The Effect of Seam Dip on the Application of the Longwall Top Coal Caving Method for Inclined Thick Seams. Ph.D. Thesis.* Sydney: The University of New South Wales; 2010.
12. Singh GSP, Singh UK. A numerical modeling approach for assessment of progressive caving of strata and performance of hydraulic powered support in longwall workings. *Comput Geotech.* 2009;36(7):1142–1156.
13. Sainsbury BA. *A Model for Cave Propagation and Subsidence Assessment in Jointed Rock Masses. Ph.D. Thesis.* Sydney: The University of New South Wales; 2012.
14. Shabanimashcool M, Li CC. Numerical modelling of longwall mining and stability analysis of the gates in a coal mine. *Int J Rock Mech Min Sci.* 2012;51(0):24–34.
15. Medhurst T, Rankine R, Kelly M. Development of a method for a longwall top coal caveability assessment. In: *Proceedings of the 14th Coal Operators' Conference.* University of Wollongong, The Australasian Institute of Mining and Metallurgy & Mine Managers Association of Australia; 2014:42–50.
16. Zhou XP, Yang HQ. Multiscale numerical modeling of propagation and coalescence of multiple cracks in rock masses. *Int J Rock Mech Min Sci.* 2012;55:15–27.
17. Cheng H, Zhou X. A multi-dimensional space method for dynamic cracks problems using implicit time scheme in the framework of the extended finite element method. *Int J Damage Mech.* 2015;24(6):859–890.
18. Silling SA. Reformulation of elasticity theory for discontinuities and long-range forces. *J Mech Phys Solids.* 2000;48(1):175–209.
19. Zhou X-P, Gu X-B, Wang Y-T. Numerical simulations of propagation, bifurcation and coalescence of cracks in rocks. *Int J Rock Mech Min Sci.* 2015;80:241–254.
20. Wang Y, Zhou X, Shou Y. The modeling of crack propagation and coalescence in rocks under uniaxial compression using the novel conjugated bond-based peridynamics. *Int J Mech Sci.* 2017;128–129:614–643.
21. Zhou XP, Bi J, Qian QH. Numerical simulation of crack growth and coalescence in rock-like materials containing multiple pre-existing flaws. *Rock Mech Rock Eng.* 2015;48(3):1097–1114.
22. Bi J, Zhou XP, Qian QH. The 3D numerical simulation for the propagation process of multiple pre-existing flaws in rock-like materials subjected to biaxial compressive loads. *Rock Mech Rock Eng.* 2016;49(5):1611–1627.
23. Bi J, Zhou X-P, Xu X-M. Numerical simulation of failure process of rock-like materials subjected to impact loads. *Int J Geomech.* 2017;17(3):04016073.
24. Itasca. *UDEC Universal Distinct Element Code v6.00 users' manual.* Minneapolis; 2014.
25. Cornah A, Vann J, Driver I. Comparison of three geostatistical approaches to quantify the impact of drill spacing on resource confidence for a coal seam (with a case example from Moranbah North, Queensland, Australia). *Int J Coal Geol.* 2013;112:114–124.
26. Gillam DJ. *Structural and Geomechanical Analysis of Naturally Fractured Hydrocarbon Provinces of the Bowen and Amadeus Basins: Onshore Australia. Ph.D. Thesis.* Adelaide: The University of Adelaide; 2004.
27. Esterle J, Sliwa R. *Bowen Basin Supermodel 2000. ACARP Project C9021.* Brisbane, Australia: CSIRO Exploration and Mining; 2002.
28. Lucas R, Neilly A, Crerar J Goonyella Riverside and Broadmeadow mine - Subsidence management plan 2015; 2015. 〈http://www.bhpbilliton.com/~/media/bhp/documents/society/regulatory/_coal/bma/goonyellariversideandbroadmeadowmines/160331_coal_bma_goonyellabroadmeadow_broadmeadowsubsidencemanagementplan.pdf?La=en〉 Accessed 16 June 2016.
29. Hoyer D. LVA version 4.1 technical features; 2010. 〈http://www.lva.com.au/documents/LVAFeatures.pdf〉 Accessed 4 April 2017.
30. International Coal News. Broadmeadow longwall production restarts after October convergence incident; 2015. 〈http://www.internationalcoalnews.com/storyView.asp?StoryID=826957978&section=News&sectionsource=s46&aspdsc=yes〉 Accessed 16 June 2016.
31. Seedsman R. *Geotechnical Assessment Goonyella exploration adit.* Brisbane, Australia: Seedsman Geotechnics Pty Ltd; 1998.
32. Shen B, Poulsen B, Kelly M, Nemcik J, Hanson C. Roadway span stability in thick seam mining - field monitoring and numerical investigation at Moranbah North mine. In: *Proceedings of the Coal Operators' Conference.* University of Wollongong; 2003:173–184.
33. Strawson C, Moodie A. Moranbah north tests the critical caving theories - every geotech engineer's dream, the ability to get more than two points on a curve. In: *Proceedings of the 26th International Conference on Ground Control in Mining.* Morgantown, WV: West Virginia University; 2007:180–187.
34. Canbulat I. Improved roadway roof support design for Anglo American Metallurgical Coals underground operations. *Min Technol.* 2011;120(1):1–13.
35. Richards BG, Coulthard MA, Toh CT. Analysis of slope stability at Goonyella Mine. *Can Geotech J.* 1981;18(2):179–194.
36. Seedsman RW, Emerson WW. The formation of planes of weakness in the highwall at Goonyella Mine, Queensland, Australia. *Eng Geol.* 1985;22(2):157–173.
37. Tarrant G. *New Concepts in Tailgate Strata Behaviour and Implications for Support Design. Ph.D. Thesis.* Sydney: University of New South Wales; 2006.
38. Gale W. Rock fracture, caving and interaction of face supports under different geological environments. Experience from Australian coal mine. In: *Proceedings of the 23rd International Conference on Ground Control in Mining.* Morgatown, WV: West Virginia University; 2004:11–19.
39. Wilson AH. The stability of underground workings in the soft rocks of the Coal Measures. *Int J Min Eng.* 1983;1(2):91–187.
40. McNally GH. Estimation of the geomechanical properties of coal measures rocks for numerical modelling. In: *Proceedings of the Symposium on Geology in Longwall Mining.* Sydney: The University of New South Wales; 1996:63–72.
41. Kwasniewski M. Numerial analysis of strata behaviour in the vicinity of a longwall panel in a coal seam mined with roof caving. In: *Proceedings of the 1st International FLAC/DEM Symposium*. Minneapolis, Minnesota: Itasca Consulting Group; 2008:07–08.
42. Vakili A, Sandy M, Albrecht J. Interpretation of non-linear numerical models in geomechanics - a case study in the application of numerical modelling for raise bored shaft design in a highly stressed and foliated rock mass. In: *Proceedings of the 6th International Conference on Mass Mining.* Sudbury, Canada; 2015: p.
43. Crowder JJ, Bawden WF. Review of post-peak parameters and behaviour of rock masses: current trends and research; 2004. 〈https://www.rocscience.com/documents/pdfs/rocnews/Fall2004.htm〉 Accessed 19 August 2015.
44. Cai M, Kaiser PK, Tasaka Y, Minami M. Determination of residual strength parameters of jointed rock masses using the GSI system. *Int J Rock Mech Min Sci.* 2007;44(2):247–265.
45. Lorig LJ, Varona P. Guidelines for numerical modelling of rock support for mines. In: *Proceedings of the 7th International Symposium on Ground Support in Mining and UndergroundConstruction.* Perth: Australian Centre for Geomechanics; 2013:81–105.
46. Sjöberg J. *Analysis of Large Scale Rock Slopes. Ph.D. Thesis.* Luleå: Luleå University of Technology; 1999.
47. Brown ET. *Block Caving Geomechanics.* Indooroopilly, Qld: Julius Kruttschnitt Mineral Research Centre, The University of Queensland; 2002.
48. Sarathchandran A. *Three Dimensional Numerical Modelling of Coal Mine Roadways Under High Horizontal Stress Fields. Master Thesis.* Exeter: University of Exeter; 2014.
49. Zhang H, He Y, Tang C, Ahmad B, Han L. Application of an improved flow-stress-damage model to the criticality assessment of water inrush in a mine: a case study. *Rock Mech Rock Eng.* 2009;42(6):911–930.
50. Bandis SC, Lumsden AC, Barton NR. Fundamentals of rock joint deformation. *Int J Rock Mech Min Sci Geomech Abstr.* 1983;20(6):249–268.
51. Bertuzzi R, Pells PJN. Geotechnical parameters of Sydney sandstone and shale. *Aust Geomech J.* 2002;37(5):41–54.
52. Le TD, Oh J, Hebblewhite B, Zhang C, Mitra R. Numerical analysis of the effect of coal seam characteristics on the longwall top coal cavability. In: *Proceedings of the 36th International Conference on Ground Control in Mining.* Morgantown, WV: Society for Mining, Metallurgy & Exploration (SME); 2017:117–123.
53. Gao F, Stead D, Coggan J. Evaluation of coal longwall caving characteristics using an innovative UDEC Trigon approach. *Comput Geotech.* 2014;55(0):448–460.

54. Kelly M, Gale W. *Ground Behavior about Longwall Faces and its Effect on Mining. ACARP Project C5017.* Brisbane, Australia: CSIRO Exploration and Mining and Strata Control Technology; 1999.
55. Brady BHG, Brown ET. *Rock Mechanics for Underground Mining*. 3rd ed. London: Kluwer Academic Publishers; 2004.
56. Kelly M, Gale WJ, Hatherly P, Balusu R, Luo X. Combining modern assessment methods to improve understanding of longwall geomechanics. In: *Proceedings of the Coal Operator's Conference*. University of Wollongong, The Australasian Institute of Mining and Metallurgy; 1998:523–535.
57. Diederichs MS, Kaiser PK. Stability of large excavations in laminated hard rock masses: the voussoir analogue revisited. *Int J Rock Mech Min Sci.* 1999;36(1):97–117.
58. Shabanimashcool M, Jing L, Li C. Discontinuous modelling of stratum cave-in in a longwall coal mine in the Arctic area. *Geotech Geol Eng.* 2014;32(5):1239–1252.
59. Mills K. Subsidence mechanisms about longwall panels. In: *Proceedings of the International Conference Geomechanics/Ground Control in Mining and Underground Construction*. Wollongong, NSW: University of Wollongong; 1998:745–756.
60. Peng SS. *Coal Mine Ground Control*. 3rd ed. Morgantown: West Virginia University; 2008.